Neuropsychopharmacology (2014) 39, 2538–2548

www.neuropsychopharmacology.org

Altered Sedative Effects of Ethanol in Mice with α1 Glycine Receptor Subunits that are Insensitive to Gβγ Modulation

Luis G Aguayo*[,1], Patricio Castro[1], Trinidad Mariqueo[1], Braulio Muñoz[1], Wei Xiong[2], Li Zhang[2], David M Lovinger[2] and Gregg E Homanics*[,3]

[1]Laboratory of Neurophysiology, Department of Physiology, University of Concepcion, Concepcion, Chile; [2]Laboratory for Integrative Neuroscience, National Institute on Alcohol Abuse and Alcoholism, National Institutes of Health, Bethesda, MD, USA; [3]Departments of Anesthesiology and Pharmacology and Chemical Biology, University of Pittsburgh, Pittsburgh, PA, USA

Alcohol abuse and alcoholism are major health problems and one of the leading preventable causes of death. Before achieving better treatments for alcoholism, it is necessary to understand the critical actions of alcohol on membrane proteins that regulate fundamental functions in the central nervous system. After generating a genetically modified knock-in (KI) mouse having a glycine receptor (GlyR) with phenotypical silent mutations at KK385/386AA, we studied its cellular and *in vivo* ethanol sensitivity. Analyses with western blotting and immunocytochemistry indicated that the expression of α1 GlyRs in nervous tissues and spinal cord neurons (SCNs) were similar between WT and KI mice. The analysis of synaptic currents recorded from KI mice showed that the glycinergic synaptic transmission had normal properties, but the sensitivity to ethanol was significantly reduced. Furthermore, the glycine-evoked current in SCNs from KI was resistant to ethanol and G-protein activation by GTP-γ-S. In behavioral studies, KI mice did not display the foot-clasping behavior upon lifting by the tail and lacked an enhanced startle reflex response that are characteristic of other glycine KI mouse lines with markedly impaired glycine receptor function. The most notable characteristic of the KI mice was their significant lower sensitivity to ethanol (~40%), expressed by shorter times in loss of righting reflex (LORR) in response to a sedative dose of ethanol (3.5 g/Kg). These data provide the first evidence to link a molecular site in the GlyR with the sedative effects produced by intoxicating doses of ethanol.
Neuropsychopharmacology (2014) **39,** 2538–2548; doi:10.1038/npp.2014.100; published online 4 June 2014

Alcohol abuse and alcoholism are major health problems that affect millions of people worldwide causing great medical and economic burdens. In the United States, for example, alcohol abuse is the third leading preventable cause of death. Ethanol is a CNS-depressant drug, and at intoxicating concentrations it disrupts most of the brain functions, including executive planning, awareness, muscle control, and memory (Spanagel, 2009). In addition, respiratory and cardiovascular functions are also affected by lethal doses of ethanol. One of the most accepted hypothesis is that ethanol interferes with neuronal membrane proteins altering their function, either excitatory or inhibitory (Jia *et al*, 2008; Lovinger *et al*, 1989; Lovinger and White, 1991; Mihic *et al*, 1997). Although it is known that inhibitory GlyRs are highly sensitive to ethanol, it is unknown how enhancement in channel activity in the presence of the drug produces the behavioral alterations resulting from its excessive consumption (Aguayo and Pancetti, 1994).

There is a large consensus that to effectively treat alcoholism new therapeutic approaches are needed. Despite the apparent efficacy of combined behavioral strategies and pharmacotherapies, less than 1/3 of alcohol-dependent patients benefit from currently available interventions (Spanagel, 2009). However, it is accepted that to efficiently develop new treatments, it is necessary to understand the critical actions of alcohol on membrane proteins that regulate fundamental functions in the central nervous system (CNS) (Vengeliene et al, 2009). This report provides the basis for a novel pharmacological role of α1 GlyRs on ethanol-induced animal behavior and defines a novel druggable molecular action based on protein–protein interactions (Azzarito *et al*, 2013; San Martin *et al*, 2012).

Here, we demonstrate that the sedative action of ethanol is related to a modulatory site in the α1 GlyR that affects channel gating by a Gβγ-dependent mechanism (Yevenes *et al*, 2008b). Using a newly generated knock-in (KI) mouse carrying a mostly behaviorally 'silent' mutation, which was previously shown to attenuate the effect of this drug on α1-containing GlyRs, we examined multiple mouse behaviors under intoxicating doses of ethanol. Our results support a critical role of the KK385–386 amino-acid residues in the sedative effects of ethanol and open the

*Correspondence: Professor LG Aguayo, Department of Physiology, University of Concepcion, PO BOX 160C, Concepcion 4030001, Chile. E-mail: laguayo@udec.cl or Professor GE Homanics, Departments of Anesthesiology and Pharmacology and Chemical Biology, University of Pittsburgh, Pittsburgh, PA, USA.
E-mail: HomanicsGE@anes.upmc.edu
Received 8 November 2013; revised 20 March 2014; accepted 21 March 2014; accepted article preview online 7 May 2014

possibility of developing specific pharmacological tools guided to interfere with this effect and perhaps other ethanol-induced behaviors.

MATERIALS AND METHODS

KI Mouse Production

A gene targeting vector was created using 8.7 kb of Strain 129S7AB2.2 mouse genomic DNA obtained from a bacterial artificial chromosome library (Source BioScience, Nottingham, UK). Recombineering (Liu *et al*, 2003), site-directed mutagenesis, and standard subcloning were used to create the targeting construct illustrated in Figure 1a. This vector was based on the strategy previously described for creating conditional KI mice (Skvorak *et al*, 2006). Details of vector construction are available from G.E.H. The linearized targeting vector was electroporated into Strain 129X1/S1-derived R1 embryonic stem (ES) cells (Nagy *et al*, 1993), and drug-resistant clones were selected as previously described (Homanics *et al*, 1997). ES cell clones were analyzed for gene targeting by Southern blotting analysis with multiple enzymes and probes (see Supplementary Figure S1). Experiments reported here were derived from clone 211H1.

Targeted ES cell clones were injected into C57BL/6J blastocysts and resulting chimeras were mated to C57BL/6J females. ES cell-derived offspring of the +/KKneo genotype (see Figure 1 for allele nomenclature) were crossed to EIIa-cre deleter mice (Lakso *et al*, 1996). The resulting heterozygous mice (+/AA) were bred to C57BL/6J to remove the cre gene from the pedigree. Subsequently,

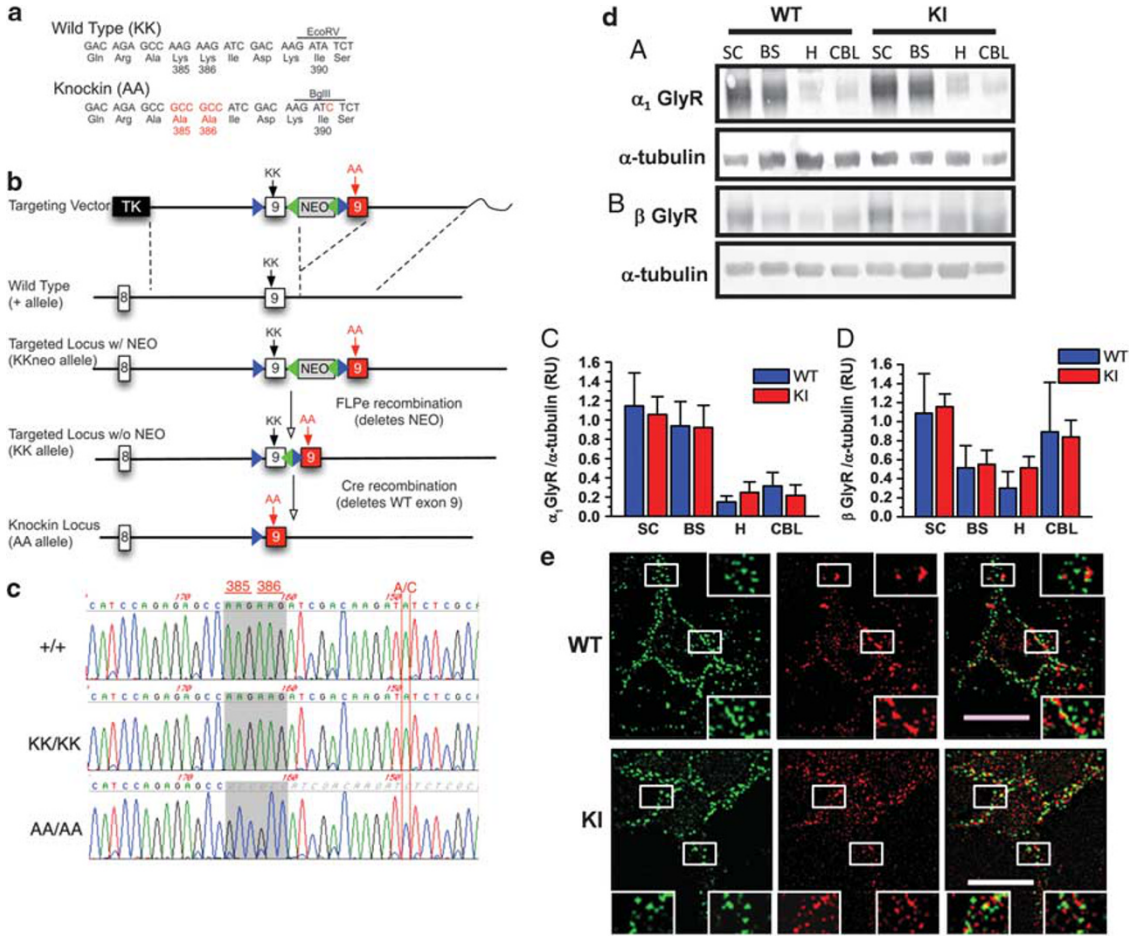

Figure 1 Gene targeting strategy. (a) Partial DNA sequence of exon 9 of the WT and KI glycine α1 receptor subunit genes. Note that the WT gene encodes lysine (K) at amino-acid positions 385–386. The KI sequence encodes alanine (A) at those amino acids. Also note the presence of a silent A to C mutation that converts an EcoRV site in the WT gene to a BglII site in the KI gene. This mutation does not change the isoleucine that is encoded at position 390. (b) Gene targeting strategy that was used to modify the glycine α1 locus. Illustrated from top to bottom are the targeting vector that was used, the endogenous WT locus, the neomycin (neo)-containing allele following gene targeting, the targeted locus following FLPe-mediated deletion of neo, and the KI locus that results from cre-mediated recombination. WT exons are depicted as white numbered boxes, whereas the mutated exon 9 is shown as a red box. Blue and green triangles represent loxP and frt sites, respectively. Black box-labeled TK represents a thymidine kinase selectable marker gene. (c) DNA sequence analysis of reverse transcription-PCR products derived from spinal cord (SC) mRNA from mice of the indicated genotypes. These results demonstrate that control mice (+/+ and KK/KK) express only the expected WT glycine α1 mRNA. In contrast, the KI mice (AA/AA) express only the expected mutations that were introduced. Panel (d) shows western blots for α1 (a) and β GlyR (b) in SC, brainstem (BS), hippocampus (H) and cerebellum (CBL) in WT and KI and summarizes the relative levels of α1 (c; $n=6$) and β (d; $n=4$) protein in both types of mice. (e) Confocal microscopy obtained in spinal neurons show the punctuated feature of α1 GlyR (green) and synaptophysin (red) in WT and KI. The squares are the magnified areas in the two neuronal genotypes. The bar represents 15 μm.

+/AA mice were interbred to produce control (+/+), heterozygous (+/AA), and homozygous KI (AA/AA) littermates. These mice consisted of a hybrid genetic background that on average, consisted of approximately 25% Strain 129X1/S1 and 75% C57BL/6J. In this report, these mice are referred to as the hybrid genetic background.

Isolation of Brainstem (BS) Neurons

Animal care and experimental protocols for this study were approved by the Institutional Animal Care and Use Committees at the Universities of Concepción, Pittsburgh and NIH and followed the guidelines for ethical protocols and care of experimental animals established by the NIH (National Institutes of Health, Maryland, USA). Mice (21–30 postnatal) were decapitated as described earlier (Jun *et al*, 2011). The brain was quickly excised, placed into cutting solution containing (in mM) sucrose 194, NaCl 30, KCl 4.5, $MgCl_2$ 1, $NaHCO_3$ 26, NaH_2PO_4 1.2, and glucose 10 (pH 7.4) saturated with 95% O_2 and 5% CO_2, glued to the chilled stage of a vibratome (Leica VT1200S, Germany), and sliced to a thickness of 400 μm. Slices were transferred to aCSF solution containing (in mM) NaCl 124, KCl 4.5, $MgCl_2$ 1, $NaHCO_3$ 26, NaH_2PO_4 1.2, glucose 10, and $CaCl_2$ 2 (pH 7.4 and 310–320 mOsm) saturated with O_2 at 30 °C for 1 h. BS slices that contained the hypoglossal nucleus were isolated and transferred to a 35-mm culture dish. Mild trituration through heat-polished pipettes was done to dissociate the tissue into single neurons. After 20 min, isolated neurons attached to the bottom of the culture dish were ready for electrophysiological experiments. Statistical analyses were performed using two-sample Kolmogorov–Smirnov test. Values of $p<0.05$ were considered statistically significant. Origin 8.0 (MicroCal) software programs were used for statistical analysis and data plots.

Spinal Cord Neuron (SCN) Cultures

Spinal neurons obtained from 5 to 6 embryos (E13–14 days, C57BL/6J) were plated at 250 000 cells/ml onto 18 mm glass coverslips coated with poly-L-lysine (350 kDa, Sigma Chemical, St Louis, MO) in plating medium for 24 h, and then the medium was replaced with feeding medium every 5 days. The neuronal feeding medium consisted of 90% minimal essential medium (MEM, GIBCO, Rockville, MD), 5% heat-inactivated horse serum (GIBCO), 5% fetal bovine serum (GIBCO) and a mixture of nutrient supplements (Aguayo and Pancetti, 1994).

Electrophysiology

Whole-cell current recordings of isolated spinal neurons and SCNs were performed using voltage-clamp (Hamill *et al*, 1981). Patch pipettes, having a 4–6 MΩ resistance, were prepared from filament-containing borosilicate micropipettes (World Precision Instruments) using a P-87 micropipette puller (Sutter Instruments). Recordings of glycine currents were done using an Axopatch 200B amplifier (Axon Instruments) at a holding potential of −60 mV. To examine the effect of ethanol on the GlyRs, we used a high concentration of intracellular Cl^-. The internal solution contained (in mM): 120 KCl, 4.0 $MgCl_2$, 10 BAPTA, 0.5 Na_2-GTP, and 2.0 Na_2-ATP (pH 7.4, 290–310 mOsmol), and the external solution contained (in mM): 150 NaCl, 5.4 KCl, 2.0 $CaCl_2$, 1.0 $MgCl_2$, 10 glucose, and 10 HEPES (pH 7.4, 300–330 mOsmol). Currents were displayed and stored on a personal computer using a 1322A Digidata. Statistical analyses were performed using the paired Student's *t*-test and ANOVA and are expressed as the mean ± SEM; values of $p<0.05$ were considered statistically significant. GraphPad Prism 5 and the Origin 8.0 (MicroCal) software programs were used for statistical analysis and data plots.

Immunocytochemistry

The spinal neurons were fixed for 3 min with cold methanol (−20 °C). After three washes with 1X PBS, neurons were blocked with normal horse serum (10%) for 30 min. Cells were incubated (overnight) with pair combination of primary antibodies: α1 GlyR (1 : 50, mouse, SySys) and synaptophysin (1 : 200, rabbit, Invitrogen). Subsequently, cells were washed with 1X PBS and incubated (2 h) with a secondary antibody rabbit anti-IgG and mouse (Cy3 and DyLight488, respectively, Jackson Labs) diluted 1 : 200 for 2 h. After five washes with 1X PBS, the preparations were mounted with Dako mounting medium (DakoCytomation, USA). Samples of spinal neurons were chosen randomly for imaging using confocal microscopy (Zeiss LSM700, Germany). Dual color immunofluorescent images were captured, stored, and analyzed using the ImageJ program (NIH) and evaluated with the Origin 6.0 program (Microcal Software Inc). Statistical analyses were performed using one-way ANOVA and are expressed as the mean ± SEM; values of $p<0.05$ were considered statistically significant.

Western Blottings

Tissue homogenates (100 μg) after detergent treatment (10 mM Tris-HCl pH 7.4, 0.25 M sucrose, 10 mM NEM, protease inhibitor cocktail 1X) were subjected to electrophoresis on 10% SDS–PAGE gels. Proteins were blotted onto nitrocellulose membrane (Bio-Rad) and blocked with 5% milk in 1X TBS-0.1% Tween 20 for 1 h with stirring. Subsequently, the membranes were incubated with primary antibodies α1GlyR (1 : 1000, mouse, SySys), βGlyR (1 : 200, mouse, SySys), and anti α-tubulin (1 : 3000, mouse, Sigma) for 1–2 h. After washes with 1X TBS and 0.1% Tween 20, membranes were incubated for 1 h with anti-mouse secondary antibodies conjugated to HRP (1 : 5000, Santa Cruz). The immunoreactivity of the proteins was detected using a chemiluminescence reagent (Promega). Levels of α-tubulin were used as loading control. Western blotting was quantified by using the 'ImageJ' (NIH) program. Statistical analyses were performed using ANOVA and are expressed as the mean ± SEM; values of $p<0.05$ were considered statistically significant.

Behavioral Characterization

Both male and female mice were used for all studies unless indicated. All mice were between 3 and 12 weeks of age at the time of testing.

Accelerating rotarod. Basal motor skill performance was tested using an accelerating rotarod assay. Briefly, mice were

placed on a non-rotating rod (Ugo Basile 7650, Varese, Italy). A timer was started when the rod began accelerating at ~14 rpm/min, and the latency to fall was recorded. Each mouse was tested 5 times on Day 1 and 10 times on Day 2. Results were analyzed with two-way repeated measures ANOVA.

Fixed speed rotarod. Mice were tested for sensitivity and tolerance to the motor ataxic effects of ethanol using a fixed speed rotarod assay. Mice were trained to remain on a rotating rotarod (8 rpm; Ugo Basile) for a maximum of 100 s for four training trials on Day 1. Subsequently, mice were injected with ethanol (2.0 g/kg; i.p.) and retested on the fixed speed rotarod at 15, 30, 45, and 60 min postinjection. On Days 2–4, all animals received a single daily injection of ethanol (2.0 g/kg). On Day 5, mice received another injection with ethanol and were tested for rotarod performance as described above. The areas over the response curves (AOC) were calculated and compared by two-way repeated measures ANOVA followed by Bonferroni *post hoc* test where appropriate.

Open field assay. Mice were tested for locomotor activity in a novel open field using automated activity monitors (Med Associates, St Albans, VT). Mice were injected with saline or ethanol (0.75, 1.0, 1.5 g/kg; i.p.) 10 min before being placed into the activity monitor. Mice were allowed to freely explore the chamber for 5 min during which time distance traveled was recorded. Results were analyzed with two-way ANOVA and Bonferonni *post hoc* test.

Hypothermia. Rectal body temperatures were recorded using a digital thermometer (Thermalert Model TH-8, probe RET-3; Physiotemp Instruments, Clifton, NJ). Temperatures were obtained before injection with ethanol (3.5 g/kg) and at 15, 30, 45, 60, 90, and 120 min postinjection. Results were analyzed with two-way repeated measures ANOVA.

LORR. Mice were tested for the sedative/hypnotic effects of ethanol (3.5 g/kg i.p.). Mice were injected with ethanol and observed for LORR. Later, mice were placed on their backs in v-shaped troughs and monitored until they were able to right themselves three times in a 30-s period. LORR was determined as the length of time from when the mouse was placed in a supine position until it was able to right itself. Results were analyzed with two-way repeated measures ANOVA.

Clearance and metabolism. Mice were administered ethanol (3.5 g/kg), and blood was collected from the tail vein at 60 and 120 min postinjection. Blood ethanol concentrations (BECs) were determined in serum/whole blood using an Analox AM1 Alcohol Analyzer (Lunenburg, MA). BECs were compared with two-way repeated measures ANOVA.

RESULTS

385/386 KI Mouse Generation

Recently, we described that an α1 subunit displaying a mutation that replaced 385/386 lysines with alanines exhibited a reduced sensitivity to ethanol (Yevenes *et al*, 2010; Yevenes *et al*, 2008a). These residues were also critical for G$\beta\gamma$-induced modulation of the GlyR (Yevenes *et al*, 2006; Yevenes *et al*, 2003). To generate a mouse line bearing this mutated glycine α1 subunit gene, standard gene targeting and ES cell technologies were used as illustrated in Figure 1a. The KI mutations that were introduced replaced the codons for lysine (K) at positions 385–386 with alanine (A). In addition, a silent mutation that did not change the codon at amino-acid 390 was also introduced for genotyping. The gene targeting approach that was used (Skvorak *et al*, 2006) created an allele that could be knocked in by cre-mediated recombination either in a conditional (tissue specific and/or temporally controlled) or global manner (Figure 1b). Mice with the conditional KI ready allele are available from the Jackson Laboratories' (Stock number 023516; Bar Harbor, ME) stock. All of the studies reported here were conducted on global KI mice that were homozygous for the KI allele (AA/AA), and these animals were compared with true WT controls (+/+).

mRNA from the spinal cord (SC) was analyzed by DNA sequence analysis of reverse transcription-PCR products. As shown in Figure 1c, +/+ and KK/KK mice expressed only mRNA that encoded lysine at positions 385–386. In contrast, AA/AA mice expressed mRNA that encoded alanine at these positions. The only other difference between the genotypes was the A/C silent mutation that was introduced for genotype analysis.

Levels of α1 GlyR protein in different areas of the CNS in WT and KI mice were compared. The western blotting data in Figure 1d show that the strongest chemiluminescence signal revealing the presence of GlyR was in the SC and BS, as compared with the hippocampus (H) and the cerebellum (CBL). Furthermore, the data show that the level of α1 GlyR was similar in WT and KI mice (Figure 1Db). Analysis of the structural β subunit in WT and KI showed similar levels. These results are in agreement with data obtained using confocal microscopy in WT and KI spinal neurons (Figure 1e, upper and lower panels, respectively). These data show that α1 GlyR (green) colocalized with synaptophysin (red), and additional quantitative analysis of α1 puncta immunoreactivity in the soma and primary processes demonstrated similar levels in WT and KI spinal neurons (Supplementary Figure S2). For example, the values for somatic puncta in WT and KI mice were 30 ± 10 and $23 \pm 4/12\,\mu m$ of neurite length ($n = 7$ neurons from three different mice each); fluorescence intensity was 56 ± 2 and 70 ± 3 RU ($n = 7$ neurons from three mice); and mean cluster size was 0.60 ± 0.03 and $0.62 \pm 0.02\,\mu m$ ($n = 7$ neurons from three mice), respectively. Together, these data suggest that the mutation of the α1 GlyR did not affect the expression of these inhibitory receptors in neurons.

The 385/386 KI Mouse Displayed Normal Glycinergic Transmission

We studied the properties of mIPSCs by recording the synaptic activity in two types of neurons; 15 DIV spinal

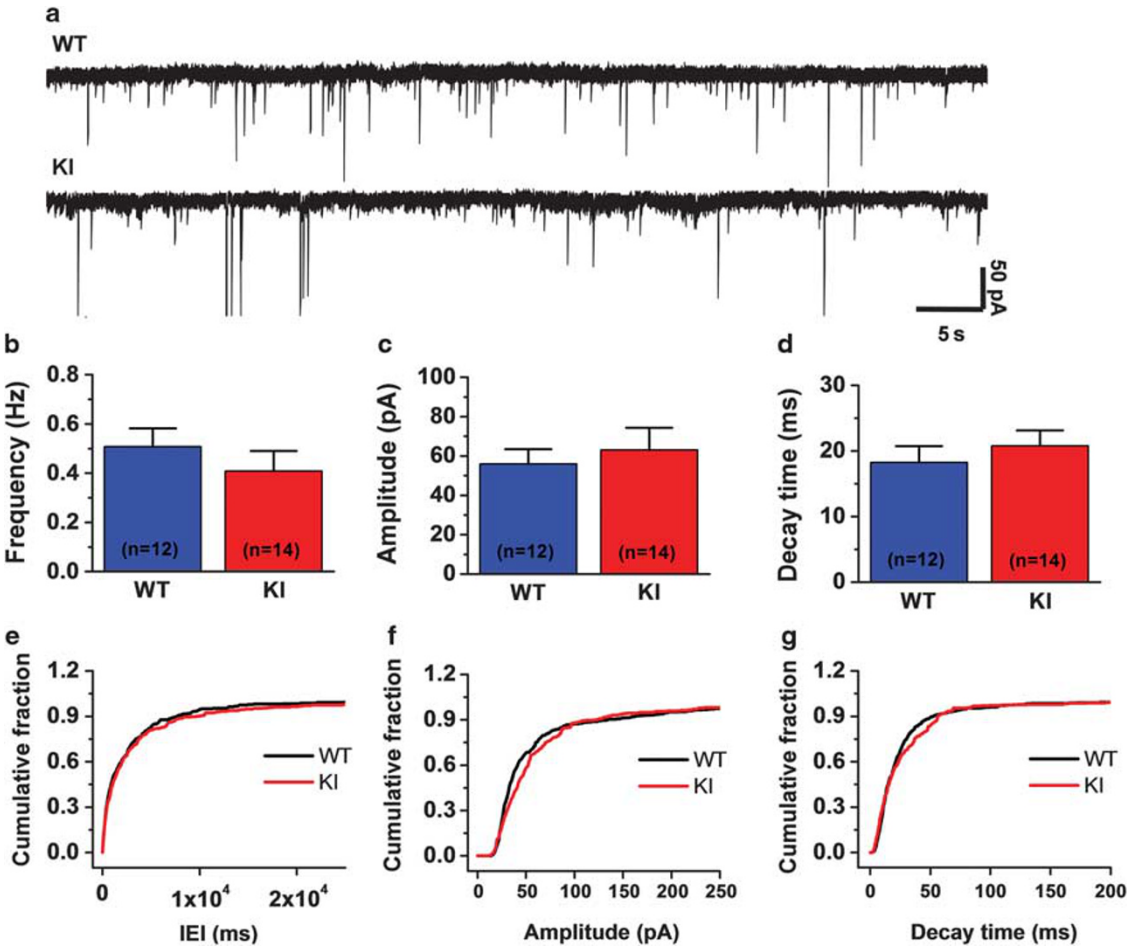

Figure 2 Properties of mIPSCs in spinal neurons from WT and KI. (a) The traces are pharmacologically isolated mIPSCs from both cell phenotypes. (b–d) Mean ± SEM for frequency, amplitude and decay time constant of mIPSCs in WT and KI mice. Panels (e–g) shows cumulative probabilities in both cell genotypes. (IEI = inter-event interval).

neurons and acutely dissociated hypoglossal neurons. The recordings were done in the presence of gabazine (5 μM) to block GABAergic transmission. Data in Figure 2 recorded in 15 DIV SCNs showed that WT and KI phenotypes had similar properties at a developmental stage when expression of α1 subunits predominate (Aguayo *et al*, 2004). For example, the values in WT ($n = 12$ neurons from 7 mice) and KI ($n = 14$ neurons, 5 mice) were very similar for frequency (0.5 ± 0.1 *vs* 0.4 ± 0.1 Hz), amplitude (56 ± 8 *vs* 63 ± 10 pA), and decay time constant (18 ± 3 *vs* 21 ± 3 ms) (Figure 2b–d). We also examined the properties of isolated glycinergic synaptic currents in mechanically isolated BS neurons (P13–18) in both WT and KI mice. sIPSCs were reversibly blocked by strychnine (1 μM), demonstrating that they were mediated by GlyRs (Supplementary Figure S3A). Comparison of these properties in WT ($n = 13$) and KI ($n = 22$) neurons showed similar average values for amplitude (111 ± 22 *vs* 120 ± 16 pA), frequency (0.2 ± 0.04 *vs* 0.3 ± 0.04 Hz), and decay time constant (16 ± 3 *vs* 17 ± 2 ms). Additional analyses with cumulative probability histograms obtained in both SCNs and BS neurons revealed no differences between the two groups (Figure 2e–g and Supplementary Figure S3B).

Effects of Ethanol on Properties of WT and KI Spinal Receptors

It was previously reported that the potentiation of GlyR by ethanol was already detected with 10 mM, a minimally intoxicating concentration (Aguayo and Pancetti, 1994). The most commonly used protocol to study ethanol on LGIC is to test with 100 mM (Aguayo and Pancetti, 1994; Guzman *et al*, 2009; Lovinger *et al*, 1989; San Martin *et al*, 2012; Yevenes *et al*, 2008b). We examined the effects of ethanol on two types of GlyR-activated inhibitory Cl^- currents, synaptically mediated mIPSCs, and macroscopic currents elicited by direct application of glycine onto spinal neurons. Ethanol significantly enhanced the decay time constant without changes in the amplitude of mIPSCs in WT neurons (Figure 3a). These data also show that although most of the cells were potentiated by ethanol, about one-third were not. On the other hand, the decay of mIPSCs recorded in KI neurons was not affected by ethanol (Figure 3b–d). For instance, overall analysis showed that the decay time constant increased by $24 \pm 2\%$ in WT in the presence of ethanol (from 18 ± 2 to 22 ± 3 ms; $n = 35$, $p < 0.05$, one-way ANOVA, Tukey's *post hoc* test), whereas

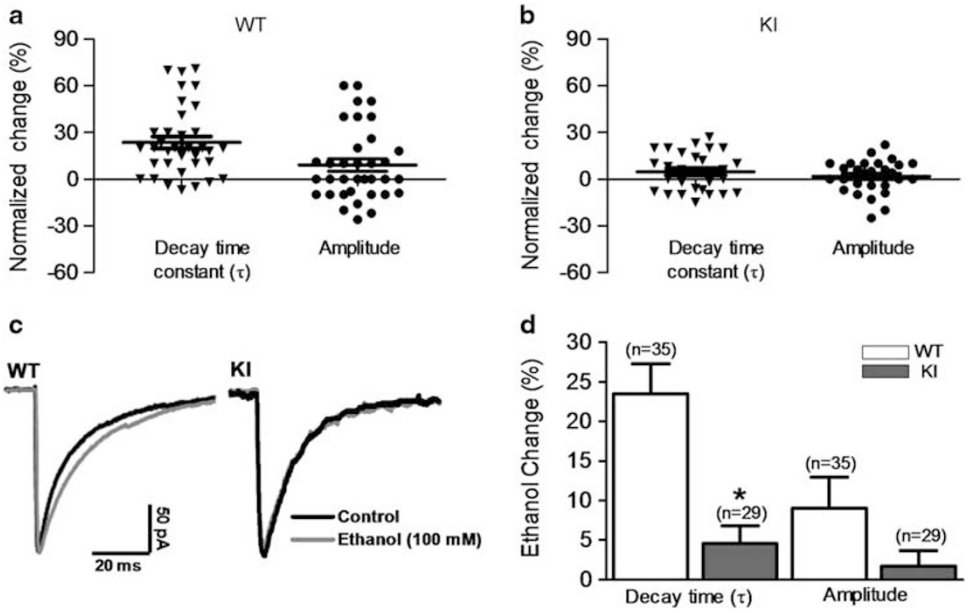

Figure 3 Attenuation of ethanol effects on glycinergic neurotransmission in KI mice. (a and b) The graph illustrates the effects of 100 mM ethanol expressed as normalized change from its own control on decay time constant and amplitude of miniature IPSCs in WT (a) and KI (b) mice. Each point represents a single neuron and the lines are mean ± SEM. (c) The traces are averaged mIPSCs before and during application of ethanol in both genotypes. (d) The data are mean ± SEM showing the effects of ethanol on decay time constant and current amplitude in WT (white bar, $n = 35$) and KI (gray bar, $n = 29$) animals. $P < 0.05$.

in KI there was no detectable increase (from 21 ± 2 to 22 ± 3 ms; $n = 29$, $p > 0.05$). Overall analyses of the two cell phenotypes showed no significant differences in current amplitude (Figure 3d, $p < 0.05$). We then examined the effect of ethanol on the current elicited by exogenously applied glycine. The agonist-evoked currents showed fairly comparable properties in WT and KI neurons, with EC_{50s} of 29 ± 3 and 23 ± 3 μM, respectively (Supplementary Table S1). Corresponding values for Hill coefficients were 1.8 ± 0.2 and 2.2 ± 0.4, respectively. In addition, the current densities were 43 ± 6 pA/pF in WT and 45 ± 6 pA/pF in KI mice (Supplementary Table S1). The current records in Figure 4a show responses evoked by an EC_{10-20} concentration of glycine and additionally show that while the current in WT neurons was potentiated by ethanol, the KI neurons were less sensitive to ethanol effects. Interestingly, experiments that examined the effect of ethanol on glycine-elicited currents showed that all of the cells were potentiated (18 of 18). Additional analysis showed that the average potentiation was $66 \pm 4\%$ in WT neurons and only $14 \pm 4\%$ in KI neurons (Figure 4b). The concentration–response curve showed that glycine-evoked currents in WT were potentiated in a concentration-dependent fashion by intoxicating levels of ethanol, but in KI mice the effects of ethanol were reduced (***$P < 0.0001$, two-way ANOVA, Tukey's *post hoc* test; Figure 4c). The data in Supplementary Table S1 summarize several properties of glycine-evoked currents and sensitivity to two general anesthetics, propofol and isoflurane, in WT and KI neurons, and the results show that they were similar, except for the modulation by ethanol. Finally, we expected that a mutation in KK385–386AA should render the receptor less sensitive to modulation by Gβγ (Yevenes *et al*, 2008b). In agreement, we found that GlyRs recorded in neurons from the KI mice were not modulated by intracellular GTP-γ-S. For example, intracellular dialysis of the guanine nucleotide for 15 min potentiated the current by $80 \pm 18\%$ in WT neurons but not in KI α1 GlyRs ($-10 \pm 12\%$, Figure 4d and e).

Motor Behavior of 385/386 KI Mice was Largely Normal

The animals studied were derived from heterozygous breeding pairs, and all genotypes were represented at weaning in numbers that were not significantly different from the predicted Mendelian ratios. KI mice were viable, healthy, had normal body weights, and were overtly indistinguishable from littermate controls. Figure 5a shows that KI mice did not display the foot clasping behavior upon lifting by the tail and lacked an enhanced startle reflex response (Figure 5b) that are characteristic of other glycine KI mouse lines with markedly impaired glycine receptor function (Borghese *et al*, 2012; Findlay *et al*, 2003a). Thus, Gβγ modulation of the glycine α1 subunit was not required for normal development and survival under the laboratory conditions in which these animals were raised.

The 385/386 KI Mouse Displayed Less Sedation and Tolerance with Ethanol

As a first approximation to characterize the behavior of the KI mice under the influence of ethanol (1.0 g/kg), we examined the distance traveled in a novel open field environment to test for locomotor activity. Total distance traveled during the 5-min test period is shown in Figure 5c. Two-way ANOVA revealed an effect of treatment ($p < 0.01$), a trend for genotype ($p = 0.059$), and an interaction of treatment with genotype ($p < 0.01$). *Post hoc* comparisons revealed that +/+ and AA/AA mice did not differ in

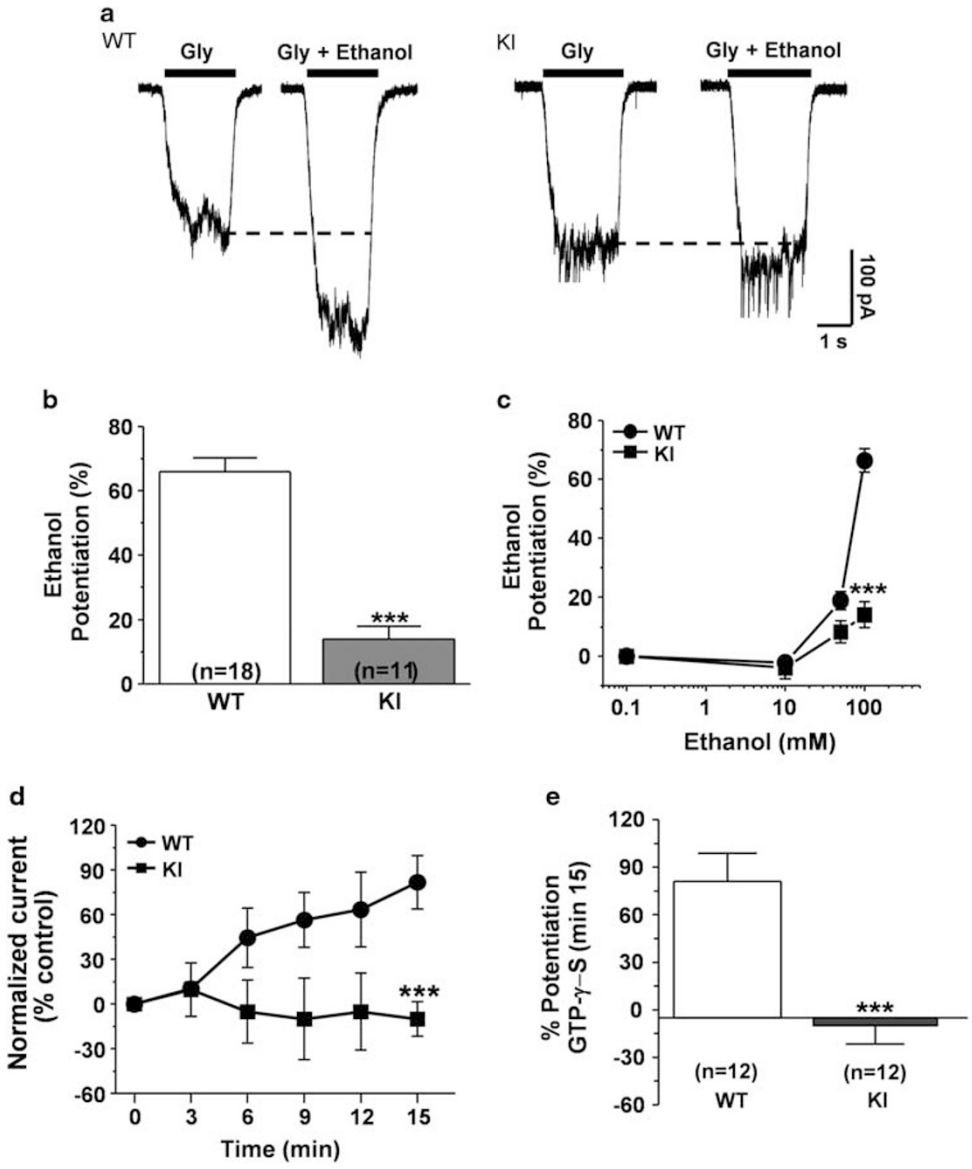

Figure 4 Effects of ethanol and GTP-γ-S on glycine-evoked Cl^- currents. (a) Current traces activated with an EC_{10} glycine and recorded in WT and KI mice neurons in the absence and presence of 100 mM ethanol. (b) The bars show the effect of ethanol on the peak current potentiation. (c) The graph illustrates concentration–response curves for WT and KI genotypes. (d) Time course of glycine current amplitude during dialysis with intracellular GTP-γ-S (0.5 mM). (e) The bars show the amplitude of the current (glycine EC_{10}) at 15 min in the presence of the nucleotide. The asterisks represent $p<0.001$.

response to the novel open field following injection with saline. In contrast to $+/+$ mice whose locomotor activity following injection with ethanol did not differ from saline, AA/AA mice responded with a significant increase in activity compared with saline ($p<0.001$).

Finally, we used a sedative dose of ethanol (3.5 g/Kg) to examine LORR. The data show that the WT and KI mice lost their reflex ability at approximately the same time after the i.p. injection (2.7 ± 0.2 *vs* 3.3 ± 0.4 min) (Supplementary Figure S4B). Interestingly, the KI mice recovered their reflex capacity much faster than the WT mice (38 ± 2, $n=12$ for WT and 23 ± 2 min, $n=11$ for KI, $^{***}p<0.001$) (Figure 5d).

Mice were tested for motor skill performance using an accelerating rotarod assay that consisted of multiple trials over a 2-day period (Supplementary Figure S4A). Two-way repeated measures ANOVA revealed a significant effect of trial ($p<0.0001$) and genotype ($p<0.005$) but no interaction of trial with genotype. Both genotypes increased performance over the course of the trials, but AA/AA mice consistently had reduced latency to fall as compared with $+/+$ controls. Thus KI mice had a small degree of impaired motor coordination.

Mice were also tested for sensitivity and tolerance to the motor ataxic effects of ethanol using a fixed speed rotarod assay (Figure 5e). Note that both genotypes were able to perform during the predrug training trials. The data show rotarod performance of $+/+$ and AA/AA mice following one or five daily injections with ethanol (2 g/kg). On Day 1, an effect of time ($p<0.0001$) but not

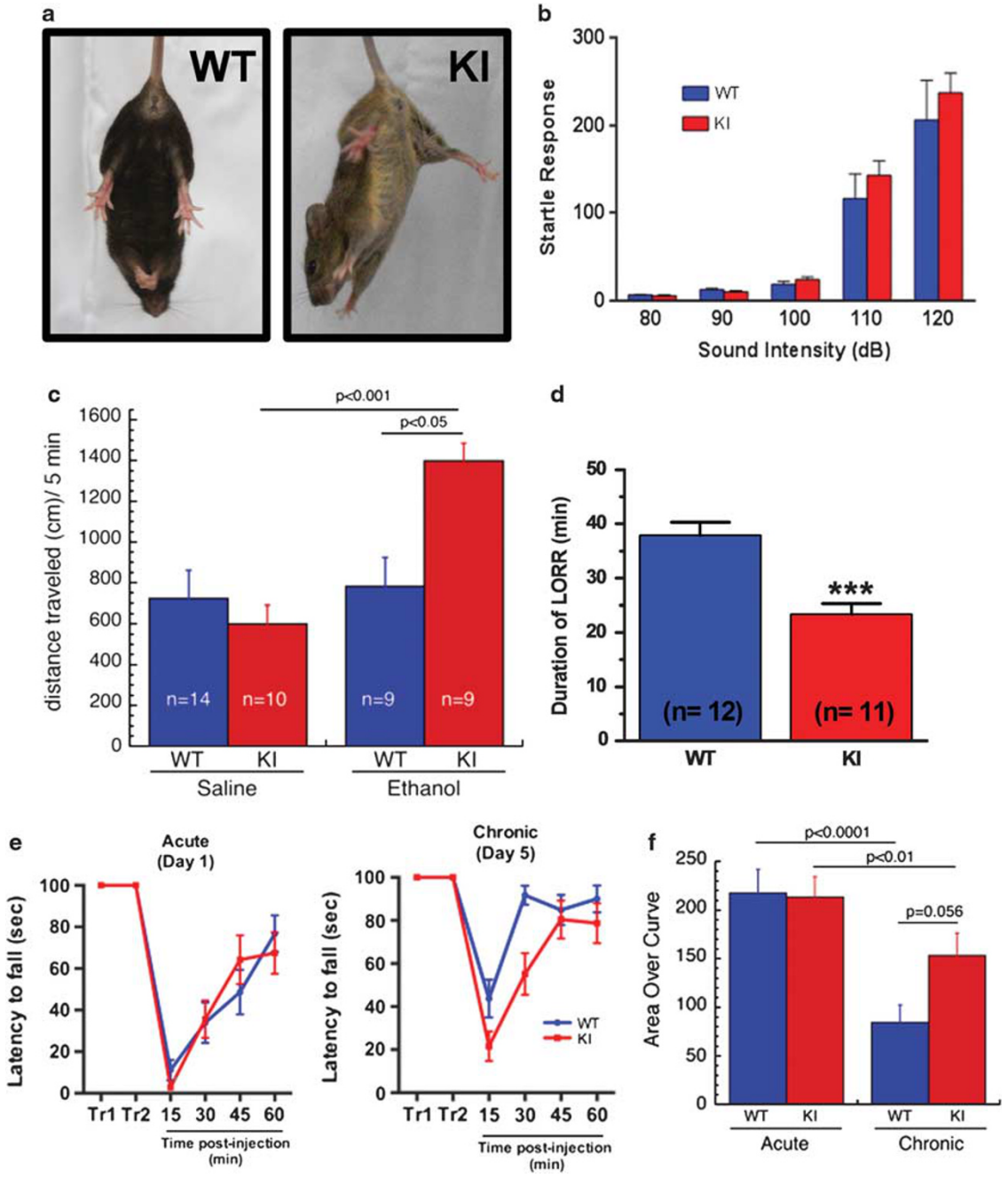

Figure 5 Ethanol produced less sedative behavior in the KI mice. (a) The KI mice did not display an increase in muscle tone as reflected by lack of limb-clenching behavior. (b) The data shows that the KI exhibited similar startle reflex behavior as the WT mice. (c) Mice were tested in an open field assay 10 min after injection of saline or ethanol (1.0 g/kg). Analysis of total distance traveled during the 5-min test period revealed no effect of ethanol in WT mice. In contrast, locomotor activity of KI mice was increased ($p<0.001$) by ethanol. (d) Duration of LORR produced by 3.5 g/kg ethanol in WT and KI mice ($P<0.05$). (e) The data shows latency to fall from a fixed speed rotarod (8 rpm) following 1 or 5 daily injections of 2.5 g/Kg ethanol. (f) Summary graph of area over the curves for the rotarod data. Both genotypes developed tolerance to daily ethanol injection, but there was a trend for reduced tolerance in KI compared with WT mice.

of genotype or interaction was observed (Figure 5e). On Day 5, an effect of time ($p<0.0001$), genotype ($p<0.05$), and an interaction ($p<0.05$) were observed. To further compare responses, AOC related to data points representing rotarod activity in the presence of ethanol was calculated and is presented in Figure 5f. Two-way repeated ANOVA measurements revealed an effect of day ($p<0.0001$) and interaction ($p\leqslant0.01$) but not of genotype. *Post hoc* analysis revealed that performance on Day 1 did not differ between genotypes. Thus KI did not alter sensitivity to the acute ataxic effects of ethanol. Following chronic exposure to ethanol, WT ($p<0.0001$) and KI ($p<0.01$) displayed a reduction in AOC, indicative of tolerance. However, AA/AA mice demonstrated a trend

toward less tolerance compared with +/+ controls ($p = 0.056$).

Mice were tested for the hypothermic effect of ethanol by measuring rectal temperatures following ethanol (3.5 g/kg) injection (Supplementary Figure S4C). Statistical analysis revealed an effect of time ($p < 0.0001$) but no effect of genotype or interaction of time with genotype. Thus ethanol induced a reduction in body temperature, but this response did not differ between genotypes.

To ensure that genotypic differences in ethanol-induced behavioral responses were not due to ethanol pharmacokinetics, BECs were determined 1 and 2 h following injection with ethanol (3.5 g/kg). At 1 h postinjection, BECs were 358 ± 6 and 362 ± 11 mg/dl for +/+ and AA/AA, respectively. At 2 h postinjection, BECs were 304.6 ± 17.7 and 299.2 ± 6.8 mg/dl for +/+ and AA/AA, respectively. Two-way repeated ANOVA measurements revealed an effect of time ($p < 0.001$) but no effect of genotype or interaction. Thus, ethanol clearance and metabolism did not differ between genotypes and cannot account for differences that were observed in behavioral assays.

DISCUSSION

This study showed that mice bearing mutations that affect the G$\beta\gamma$-dependent allosteric modulation of GlyRs (Yevenes *et al*, 2006) displayed a significant reduction in LORR induced by an intoxicating dose of ethanol. The KI mice behaved normally (Figure 5a and b) and exhibited unchanged levels of neuronal GlyRs (Figure 1) and metabolism of ethanol. However, we found a significant difference on open field exploration with a low concentration of ethanol (Figure 5c). The increase in locomotor activity in the KI mice might have resulted from neuronal disinhibition resulting from the reduced effect of ethanol on GlyR. In the WT mice, on the other hand, the ethanol-sensitive GlyR was able to provide a high level of inhibition counteracting an excitatory pathway, the nature of which is currently unknown. Yet, the most relevant result was the reduced time of LORR linking the insensitivity of α1-containing GlyRs to a sedative action of ethanol (Figure 5d). The electrophysiological data obtained in SCNs and isolated BS neurons revealed similar properties in WT and KI (Figure 2, Supplementary Figure S3), with KI neurons being primarily resistant to ethanol in both mIPSC (Figure 3) and glycine-evoked current (Figure 4).

Glycine receptors, like $GABA_A$Rs, serotonin type 3 receptors, and nicotinic acetylcholine receptors, belong to the Cys-loop ligand gated ion channel superfamily (Thompson *et al*, 2010). They share several structural similarities such as the presence of a large N-terminal extracellular domain with the ligand binding site, four transmembrane segments (TM1–4) with the pore formed by TM2, and one large intracellular loop (IL) connecting TM3 and TM4 that participates in several modulatory mechanisms (Melzer *et al*, 2010; Specht *et al*, 2011; Unwin, 2003).

It is currently accepted that glycinergic neurotransmission is critical for a series of neural functions, and alterations in this main inhibitory mechanism resulting from blockade of postsynaptic receptors, mutations in glycine-associated proteins, and inhibition of glycine reuptake have profound effects on neuronal excitability, resulting in muscle spasticity and hyper reflexia that are of clinical relevance (Davies *et al*, 2010; Dutertre *et al*, 2012). For example, hyperekplexia is a neuromotor disorder characterized by exaggerated startle reflexes and hypertonia in response to sudden, unexpected auditory or tactile stimuli. This disorder, which is potentially fatal, is primarily caused by inherited mutations in the genes encoding the GlyR α1 subunit (GLRA1) and the presynaptic glycine transporter GlyT2 (SLC6A5) (Carta *et al*, 2012). However, mutations have also been discovered in the genes encoding the GlyR β subunit (GLRB) (Chung *et al*, 2012).

In addition, previous studies showed that G$\beta\gamma$ association contributes to the allosteric effect of ethanol on GlyR channel gating (Yevenes *et al*, 2006), where the participation of residues KK385–386 in the IL are most relevant (Yevenes *et al*, 2008b). These residues are important for the effects of ethanol on the GlyR, which are reversible and associated with a leftward shift in the concentration–response curve (ie, increase in apparent affinity) (Aguayo, 1996). Therefore, understanding the molecular actions of ethanol on the GlyR is relevant to human health and, in this respect, the present study demonstrates that the sedation induced by ethanol is linked to the allosteric potentiation of the GlyR.

It is important to discuss the present results in relation to other previous studies that suggested that binding sites in TM regions in GlyRs are important for ethanol actions. Additionally, a critical amino acid in loop 2 of the extracellular domain, A52, was reported to modulate ethanol sensitivity in the receptor (Perkins *et al*, 2009). We believed that because mice genetically engineered to display an ethanol-resistant GlyR based on sites in TM regions exhibited hypo functional receptors and were hyper excitable, the interpretation about ethanol's site and mechanism of action was confounded (Findlay *et al*, 2003b). The KI mice, on the other hand, although overtly normal in broad behavior, were less sedated by ethanol, indicating that this depressing action of ethanol is, in part, mediated by glycinergic neurotransmission. The results also show that the modulation of the glycinergic transmission by G$\beta\gamma$ was important in higher levels of network activity. Consistent with its localization and roles in motor control, the KI mouse showed a degree of impairment in the accelerating rotarod assay (Supplementary Figure S4A). Thus, the GlyR G$\beta\gamma$ interaction appears to be important for neuronal control under a high level of inhibitory demand. At the cellular level, this appears to be correlated with an increased level of receptor function, as evidenced by a slight increase in the decay time constant and apparent affinity (EC_{50}) of GlyR in the KI mice (Supplementary Table S1).

Glycine is the main inhibitory neurotransmitter present in the SC and BS and has significant roles in motor and respiratory control mechanisms (Legendre, 2001; Lynch, 2004). In the mature CNS, glycine activates mainly GlyRs composed of α1 and β subunits (Aguayo *et al*, 2004). Interestingly, Cl^--permeable GlyRs are one of the most sensitive ethanol molecular targets in the CNS, providing a neurobiological basis for its depressing effects on motor

control, cardiovascular regulation, and sedation (Chang and Martin, 2011; Krowicki and Kapusta, 2011; Ren and Greer, 2006; Schmid *et al*, 1991). In addition, because recent studies showed that GlyRs are also found in supra spinal regions, such as VTA and nucleus accumbens, it is possible to postulate that they might be implicated in reward and ethanol-seeking behaviors (Chau *et al*, 2010; Li *et al*, 2012). Thus the present study opens the possibility of relating spinal and BS inhibition to the sedation caused by this drug of abuse. Because the α2 subunit of the GlyR also presents the G$\beta\gamma$-binding sequence (Yevenes *et al*, 2010), it seems possible that these supra spinal receptors are also affected by a similar ethanol mechanism.

In conclusion, the present results strongly suggest an important function of α1 GlyR on sedative effects of ethanol and confirms the role of KK385–386 residues in these effects. Furthermore, these KI mice can be a new tool for alcohol addiction studies, not only in motor areas associated with sedative actions like BS and SC but also in other important regions for reward like nucleus accumbens and VTA.

FUNDING AND DISCLOSURE

The authors declare no conflict of interest.

ACKNOWLEDGEMENTS

We thank Carolyn Ferguson and Lauren J Aguayo for expert technical assistance. This work was supported by an NIH grant AA17875 awarded to LGA and GEH. The work of WX, LZ and DML was supported by the Division of Intramural Clinical and Biological Research of NIAAA. All reagents and materials used for this work are commercially available.

REFERENCES

Aguayo LG (1996). Potentiation of the glycine-activated Cl^- current by ethanol in cultured mouse spinal neurons. *J Pharmacol Exp Ther* **279**: 1116–1122.

Aguayo LG, Pancetti FC (1994). Ethanol modulation of the γ-aminobutyric $acid_A$- and glycine-activated Cl^- current in cultured mouse neurons. *J Pharmacol Exp Ther* **270**: 61–69.

Aguayo LG, van Zundert B, Tapia JC, Carrasco MA, Alvarez FJ (2004). Changes on the properties of glycine receptors during neuronal development. *Brain Res Rev* **47**: 33–45.

Azzarito V, Long K, Murphy NS, Wilson AJ (2013). Inhibition of alpha-helix-mediated protein-protein interactions using designed molecules. *Nat Chem* **5**: 161–173.

Borghese CM, Blednov YA, Quan Y, Iyer SV, Xiong W, Mihic SJ *et al* (2012). Characterization of two mutations, M287L and Q266I, in the α1 glycine receptor subunit that modify sensitivity to alcohols. *J Pharmacol Exp Ther* **340**: 304–316.

Carta E, Chung SK, James VM, Robinson A, Gill JL, Remy N *et al* (2012). Mutations in the GlyT2 gene (SLC6A5) are a second major cause of startle disease. *J Biol Chem* **287**: 28975–28985.

Chang Q, Martin LJ (2011). Glycine receptor channels in spinal motoneurons are abnormal in a transgenic mouse model of amyotrophic lateral sclerosis. *J Neurosci* **31**: 2815–2827.

Chau P, Höifödt-Lidö H, Löf E, Söderpalm B, Ericson M (2010). Glycine receptors in the nucleus accumbens involved in the ethanol intake-reducing effect of acamprosate. *Alcohol Clin Exp Res* **34**: 39–45.

Chung SK, Bode A, Cushion TD, Thomas RH, Hunt C, Wood SE *et al* (2012). GLRB is the third major gene of effect in hyperekplexia. *Hum Mol Genet* **22**: 927–940.

Davies JS, Chung SK, Thomas RH, Robinson A, Hammond CL, Mullins JG *et al* (2010). The glycinergic system in human startle disease: a genetic screening approach. *Front Mol Neurosci* **3**: 8.

Dutertre S, Becker CM, Betz H (2012). Inhibitory glycine receptors: an update. *J Biol Chem* **287**: 40216–40223.

Findlay GS, Phelan R, Roberts MT, Homanics GE, Bergeson S, Lopreato G *et al* (2003a). Glycince receptor knock-in mutant mice exhibit a more dramatic hyperekplexia-like phenotype compared to a null mutation. *J Neurosci* **23**: 8051–8059.

Findlay GS, Phelan R, Roberts MT, Homanics GE, Bergeson SE, Lopreato GF *et al* (2003b). Glycine receptor knock-in mice and hyperekplexia-like phenotypes: comparisons with the null mutant. *J Neurosci* **23**: 8051–8059.

Guzman L, Moraga-Cid G, Avila A, Figueroa M, Yevenes GE, Fuentealba J *et al* (2009). Blockade of ethanol-induced potentiation of glycine receptors by a peptide that interferes with G binding. *J Pharmacol Exp Ther* **331**: 933–939.

Hamill OP, Marty A, Neher E, Sakmann B, Sigworth FJ (1981). Improved patch-clamp techniques for high-resolution current recording from cells and cell-free membrane patches. *Pflugers Arch* **391**: 85–100.

Homanics GE, Ferguson C, Quinlan JJ, Daggett J, Snyder K, Lagenaur C *et al* (1997). Gene knockout of the α6 subunit of the γ-aminobutyric acid type A receptor: lack of effect on responses to ethanol, pentobarbital, and general anesthetics. *Mol Pharmacol* **51**: 588–596.

Jia F, Chandra D, Homanics GE, Harrison NL (2008). Ethanol modulates synaptic and extrasynaptic GABAA receptors in the thalamus. *J Pharmacol Exp Ther* **326**: 475–482.

Jun SB, Cuzon Carlson V, Ikeda S, Lovinger D (2011). Vibrodissociation of neurons from rodent brain slices to study synaptic transmission and image presynaptic terminals. *J Vis Exp* **51**: 2752.

Krowicki ZK, Kapusta DR (2011). Microinjection of glycine into the hypothalamic paraventricular nucleus produces diuresis, natriuresis, and inhibition of central sympathetic outflow. *J Pharmacol Exp Ther* **337**: 247–255.

Lakso M, Pichel JG, Gorman JR, Sauer B, Okamoto Y, Lee E *et al* (1996). Efficient in vivo manipulation of mouse genomic sequences at the zygote stage. *Proc Natl Acad Sci USA* **93**: 5860–5865.

Legendre P (2001). The glycinergic inhibitory synapse. *Cell Mol Life Sci* **58**: 760–793.

Li J, Nie H, Bian W, Dave V, Janak PH, Ye JH (2012). Microinjection of glycine into the ventral tegmental area selectively decreases ethanol consumption. *J Pharmacol Exp Ther* **341**: 196–204.

Liu P, Jenkins NA, Copeland NG (2003). A highly efficient recombineering-based method for generating conditional knockout mutations. *Genome Res* **13**: 476–484.

Lovinger D, White G, Weight F (1989). Ethanol inhibits NMDA-activated ion current in hippocampal neurons. *Science* **243**: 1721–1724.

Lovinger DM, White G (1991). Ethanol potentiation of 5-hydroxytryptamine 3 receptor-mediated ion current in neuroblastoma cells and isolated adult mammalian neurons. *Mol Pharmacol* **40**: 263–270.

Lynch JW (2004). Molecular structure and function of the glycine receptor chloride channel. *Physiol Rev* **84**: 1051–1095.

Melzer N, Villmann C, Becker K, Harvey K, Harvey RJ, Vogel N *et al* (2010). Multifunctional basic motif in the glycine receptor intracellular domain induces subunit-specific sorting. *J Biol Chem* **285**: 3730–3739.

Mihic SJ, Ye Q, Wick MJ, Koltchine VV, Krasowski MD, Finn SE *et al* (1997). Sites of alcohol and volatile anaesthetic action on GABA(A) and glycine receptors. *Nature* **389**: 385–389.

Nagy A, Rossant J, Nagy R, Abramow-Newerly W, Roder JC (1993). Derivation of completely cell culture-derived mice from early-passage embryonic stem cells. *Proc Natl Acad Sci USA* **90**: 8424–8428.

Perkins DI, Trudell JR, Crawford DK, Asatryan L, Alkana RL, Davies DL (2009). Loop 2 structure in glycine and GABAA receptors plays a key role in determining ethanol sensitivity. *J Biol Chem* **284**: 27304–27314.

Ren J, Greer JJ (2006). Modulation of respiratory rhythmogenesis by chloride-mediated conductances during the perinatal period. *J Neurosci* **26**: 3721–3730.

San Martin L, Cerda F, Jimenez V, Fuentealba J, Munoz B, Aguayo LG *et al* (2012). Inhibition of the ethanol-induced potentiation of alpha1 glycine receptor by a small peptide that interferes with Gbetagamma binding. *J Biol Chem* **287**: 40713–40721.

Schmid K, Bohmer G, Gebauer K (1991). Glycine receptor-mediated fast synaptic inhibition in the brainstem respiratory system. *Respir Physiol* **84**: 351–361.

Skvorak K, Vissel B, Homanics GE (2006). Production of conditional point mutant knockin mice. *Genesis* **44**: 345–353.

Spanagel R (2009). Alcoholism: a systems approach from molecular physiology to addictive behavior. *Physiol Rev* **89**: 649–705.

Specht CG, Grunewald N, Pascual O, Rostgaard N, Schwarz G, Triller A (2011). Regulation of glycine receptor diffusion properties and gephyrin interactions by protein kinase C. *EMBO J* **30**: 3842–3853.

Thompson AJ, Lester HA, Lummis SCR (2010). The structural basis of function in Cys-loop receptors. *Q Rev Biophys* **43**: 449–499.

Unwin N (2003). Structure and action of the nicotinic acetylcholine receptor explored by electron microscopy. *FEBS Lett* **555**: 91–95.

Vengeliene V, Bilbao A, Molander A, Spanagel R (2009). Neuropharmacology of alcohol addiction. *Br J Pharmacol* **154**: 299–315.

Yevenes GE, Moraga-Cid G, Avila A, Guzman L, Figueroa M, Peoples RW *et al* (2010). Molecular requirements for ethanol differential allosteric modulation of glycine receptors based on selective Gbetagamma modulation. *J Biol Chem* **285**: 30203–30213.

Yevenes GE, Moraga-Cid G, Guzman L, Haeger S, Oliveira L, Olate J *et al* (2006). Molecular determinants for G protein beta modulation of ionotropic glycine receptors. *J Biol Chem* **281**: 39300–39307.

Yevenes GE, Moraga-Cid G, Peoples RW, Schmalzing G, Aguayo LG (2008a). A selective G betagamma-linked intracellular mechanism for modulation of a ligand-gated ion channel by ethanol. *Proc Natl Acad Sci USA* **105**: 20523–20528.

Yevenes GE, Moraga-Cid G, Peoples RW, Schmalzing G, Aguayo LG (2008b). A selective G -linked intracellular mechanism for modulation of a ligand-gated ion channel by ethanol. *Proc Natl Acad Sci* **105**: 20523–20528.

Yevenes GE, Peoples RW, Tapia JC, Parodi J, Soto X, Olate J *et al* (2003). Modulation of glycine-activated ion channel function by G-protein betagamma subunits. *Nat Neurosci* **6**: 819–824.

Supplementary Information accompanies the paper on the Neuropsychopharmacology website (http://www.nature.com/npp)